ChemComm
Chemical Communications

Accepted Manuscript

This article can be cited before page numbers have been issued, to do this please use: P. Siekierski, E. Michaltsis, J. Schleisiek, N. Montesdeoca and J. Karges, *Chem. Commun.*, 2025, DOI: 10.1039/D5CC05177K.

ROYAL SOCIETY OF CHEMISTRY

rsc.li/chemcomm

ChemComm

View Article Online
DOI: 10.1039/D5CC05177K

COMMUNICATION

Red-Light Excitation of a Ru(II)-Pt(II) Tetranuclear Complex for Combined Photoactivated Chemotherapy and Photodynamic Therapy

Received 00th January 20xx,
Accepted 00th January 20xx

DOI: 10.1039/x0xx00000x

Pia Siekierski,[a] Eleni Michaltsis,[a] Julia Schleisiek,[a] Nicolás Montesdeoca,[a] Johannes Karges,*[a]

We report the synthesis and biological evaluation of a tetranuclear Ru(II)-Pt(II) complex activated by red light (630 nm). Upon irradiation, the Ru(II) center photo-catalytically generates singlet oxygen while simultaneously releasing Pt(II) moieties, thereby inducing a multimodal therapeutic effect in cancer cells by photodynamic therapy and photoactivated chemotherapy.

Light-activated therapeutics have attracted increasing attention in recent years due to their ability to provide precise spatial and temporal control over treatment.[1-3] Among the most promising strategies are photodynamic therapy (PDT) and photoactivated chemotherapy (PACT). In both approaches, a photoresponsive compound is administered either locally or systemically. After a defined incubation period, the targeted tissue is exposed to light irraidation, causing the therapeutic effect in a highly localized manner. In PDT, irradiation leads to the catalytic generation of reactive oxygen species (ROS), most notably singlet oxygen, which induces cell death. In contrast, PACT relies on the light-induced release of a therapeutically active molecule, such as a cytotoxic metal center or small molecular agent. Importantly, in both cases, the therapeutic action is confined to the irradiated region containing the photoactive agent, offering the potential for selective and minimally invasive cancer treatment. Despite these advantages, both methods face intrinsic limitations. The efficacy of PDT is strongly dependent on the availability of oxygen in the targeted tissue, which is often severely restricted in hypoxic tumor environments.[4, 5] PACT, on the other hand, requires stoichiometric amounts of the photoactive compound, which may limit its therapeutic efficiency.[6, 7] To overcome these challenges, recent research has increasingly focused on the development of multimodal systems that combine the catalytic features of PDT with the molecular release mechanism of PACT, aiming to achieve therapeutic outcomes with improved efficacy.[8]

Herein, the chemical synthesis, photophysical characterization, and biological evaluation of a novel tetranuclear Ru(II)–Pt(II) complex is reported. Upon irradiation, Pt(II) groups are released, resulting in a multimodal effect. The Pt(II) species accumulated in the nucleus, eliciting a chemotherapeutic response, while the Ru(II) moiety acted as a photosensitizer to generate singlet oxygen within the cytoplasm. Owing to this combined mechanism, the tetranuclear Ru(II)–Pt(II) complex exhibited broad phototoxicity across various cancer cell lines in the micromolar range.

The Ru(II) precursor [Ru(dimethyl sulfoxide)$_4$(Cl)$_2$] was synthesized by reducing Ru(III) chloride to Ru(II) in ethanol and saturating the open coordination sites with dimethyl sulfoxide. A mixture of [Ru(dimethyl sulfoxide)$_4$(Cl)$_2$] and silver(I) trifluoromethanesulfonate was then dissolved in ethanol and heated to reflux for 3 h. The resulting insoluble silver(I) chloride was filtered off, and the solution of the Ru(II) precursor was transferred to a glass syringe. Separately, an excess of the ligand 2,2'-bipyrimidine was dissolved in ethanol and heated to reflux. The Ru precursor solution was added slowly to the ligand solution over 20 h using a syringe pump. Afterward, sodium tetraphenylborate was added, and the desired product was isolated as a tetraphenylborate salt. Finally, the Ru(II) polypyridine complex [Ru(2,2'-bipyrimidine)$_3$][Cl]$_2$ (**Ru**) was obtained as the chloride salt using the Amberlite IR-410 ion exchange resin. The Pt(II) precursor [Pt(dimethyl sulfoxide)$_2$(Cl)$_2$] was prepared upon treatment of potassium tetrachloridoplatinate with silver(I) trifluoromethanesulfonate as previously reported.[9] [Pt(dimethyl sulfoxide)$_2$(Cl)$_2$] and 2,2'-bipyrimidine were combined in equimolar amounts in methanol and heated to reflux for 4 h. The product [Pt(2,2'-bipyrimidine)(Cl)$_2$] (**Pt**) was isolated in high yield by recrystallization. Separately, [Ru(dimethyl sulfoxide)$_4$(Cl)$_2$] was mixed with silver(I) trifluoromethanesulfonate, and the resulting silver(I) chloride was removed by filtration. The solution of the Ru(II) precursor was then slowly added over 20 h to a solution of [Pt(2,2'-bipyrimidine)(Cl)$_2$] using a syringe pump. The final product [Ru(Pt(2,2'-bipyrimidine)(Cl)$_2$)$_3$][Cl]$_2$ (**RuPt**) was obtained by

[a] Faculty of Chemistry and Biochemistry, Ruhr-University Bochum, Universitätsstrasse 150, 44780 Bochum, Germany
* E-Mail: johannes.karges@ruhr-uni-bochum.de, Tel: +49 2343224187; WWW: www.kargesgroup.ruhr-uni-bochum.de
Supplementary Information available: [details of any supplementary information available should be included here]. See DOI: 10.1039/x0xx00000x

recrystallization (Figure 1). The identity of the tetranuclear metal complex was verified by high-pressure liquid chromatography (HPLC) as well as high-resolution matrix-assisted laser desorption ionization time of flight mass spectrometry analyses (calcd. for $C_{24}H_{18}Cl_7N_{12}Pt_3Ru$ $[M\text{-}Cl]^+$ m/z 1405.7584; found: 1405.7591). All compounds were characterized by nuclear magnetic resonance spectroscopy and mass spectrometry, and the purity of the final products was confirmed by elemental analysis (Figure S1–S10).

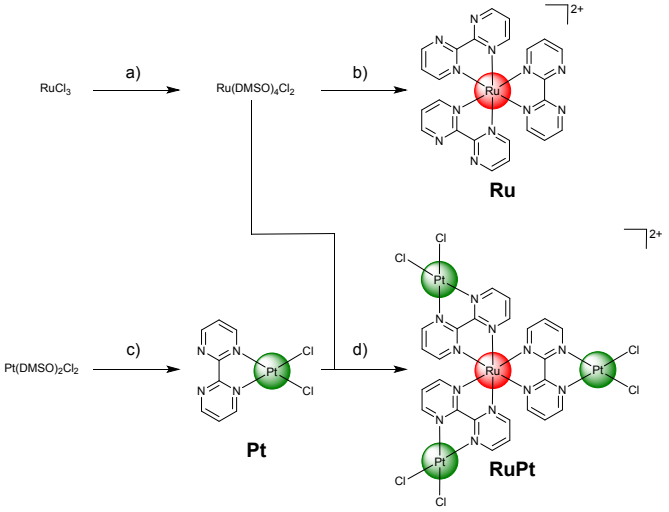

Figure 1. Schematic illustration of the strategy for the synthesis of the herein studied metal complexes. The complexes were isolated as chloride salts. a) 1. ethanol, reflux, 3 h; 2. dimethyl sulfoxide, 150 °C, 2 h; b) 1. silver(I) trifluoromethanesulfonate ethanol, reflux, 3 h; 2. 2,2'-bipyrimidine, ethanol, reflux, syringe pump, 20 h; c) 2,2'-bipyrimidine, methanol, reflux, 4h; d) 1. silver(I) trifluoromethanesulfonate ethanol, reflux, 3 h; 2. [Pt(2,2'-bipyrimidine)$(Cl)_2$], isopropanol/octanol, reflux, syringe pump, 20 h.

Based on the rich photophysical properties of Pt(II) and Ru(II) polypyridine complexes, the absorption profile of the mononuclear and tetranuclear metal complexes in water was examined. The Pt(II) complex **Pt** showed a strong absorption peak in the ultraviolet region with an absorption tail reaching into the blue region. This absorption profile is in agreement with previous reports of Pt(II) bipyridine-type complexes.[10] The Ru(II) polypyridine complex **Ru** had an absorption maximum in the ultraviolet region, typically corresponding to ligand-centered transitions. In addition, the metal complex showed a absorption peaks in the blue region corresponding to metal-ligand charge transfer transitions, which is in agreement with the previous literature of Ru(II) polypyridine complexes.[11] Interestingly, the compound had an absorption tail reaching into the red region of the spectrum. In comparison to that, the tetranuclear metal complex **RuPt** had an absorption maximum in the ultraviolet region (250 nm: $\varepsilon = 267.3 \times 10^3\ M^{-1}\ cm^{-1}$) as well as serval absorption bands centered at 365 nm ($\varepsilon = 77.1 \times 10^3\ M^{-1}\ cm^{-1}$) and 505 nm ($\varepsilon = 31.2 \times 10^3\ M^{-1}\ cm^{-1}$). Strikingly, the compound had a long absorption tail reaching into the red and near-infrared region up to approximately 880 nm of the spectrum (exemplary 630 nm: $\varepsilon = 11.8 \times 103\ M^{-1}\ cm^{-1}$; 800 nm: $\varepsilon = 2.6 \times 10^3\ M^{-1}\ cm^{-1}$). Notably, previous studies have demonstrated that photosensitizers can remain active even with extinction coefficients below 100 $M^{-1}\ cm^{-1}$.[12] These findings indicate that the compound might be excitable with red or near-infrared light (Figure 2).

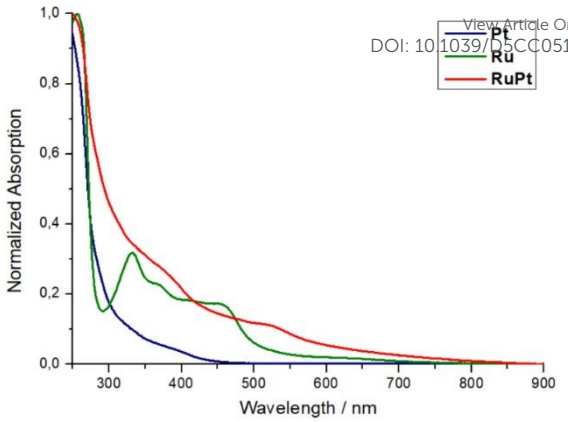

Figure 2. Normalized absorption spectra of **Ru**, **Pt**, and **RuPt** in water.

To gain a deeper insight into the photophysical properties of the complexes **Pt**, **Ru**, and **RuPt**, density functional theory (DFT) calculations of the electronic singlet ground states were computed. The results provided details of the localization and energies of the highest occupied molecular orbital (HOMO) and the lowest unoccupied molecular orbital (LUMO). For **Pt**, both the HOMO and LUMO were predominantly localized at the 2,2'-bipyrimidine moiety (Figure 3A), indicating ligand-centered (LC) transitions in the ultraviolet region, as observed in the experimental spectrum (Figure 2). In contrast, the HOMO of the tris-2,2'-bipyrimidine **Ru** complex was metal-centered on the d-orbitals of the ruthenium center. The LUMO was localized on the π^* orbitals of the ligands (Figure 3B), resulting in metal-to-ligand charge transfer (MLCT), consistent with previously reported ruthenium polypyridyl complexes. By combining the **Pt** and **Ru** complexes into the tetranuclear complex **RuPt**, the localization of the HOMO and LUMO showed a shift in orbital distribution (Figure 3C). Interestingly, the HOMO was mainly localized on the platinum rather than on the d-orbitals of ruthenium. This observation could be explained by the electronic differences of the metals, as the higher lying 5d orbitals of platinum promote the HOMO localization on platinum rather than on the 4d orbitals of ruthenium. Furthermore, the calculations revealed that the HOMO of **Ru** had an energy of -6.98 eV, compared to -7.37 eV for **RuPt**, indicating a slightly more stabilized HOMO in the tetranuclear complex. Also, the energies of the HOMO-4 to HOMO-1 levels of **RuPt** were almost degenerated (Table S1), indicating delocalization over multiple platinum centers and further stabilization of the HOMO. Additionally, the LUMO of **RuPt** was also lower in energy than that of **Ru** (-4.03 eV vs. 3.11 eV). In contrast, the localization of the LUMO remained predominantly localized on the π^* orbitals of the 2,2'-bipyrimidine ligands, consistent with the behavior previously observed in **Pt** and **Ru**. Capitalizing on this, the bridging of the 2,2'-bipyrimidine ligands between ruthenium and platinum may contribute to the LUMO stabilization in **RuPt** through MLCT interactions. Moreover, combining ruthenium and platinum resulted in a decreased HOMO-LUMO gap, from $\Delta E = 3.87$ eV in **Ru** to $\Delta E = 3.34$ eV in **RuPt**. Based on the previously described changes in the localization and energies of the HOMO and LUMO, it can be hypothesized that these altered electronic effects might contribute to the experimentally observed long bathochromic absorption tail, as indicated by the absorption spectra of **RuPt** in Figure 2 (coordinates of compounds: Table S2-S4).

View Article Online
DOI: 10.1039/D5CC00527K

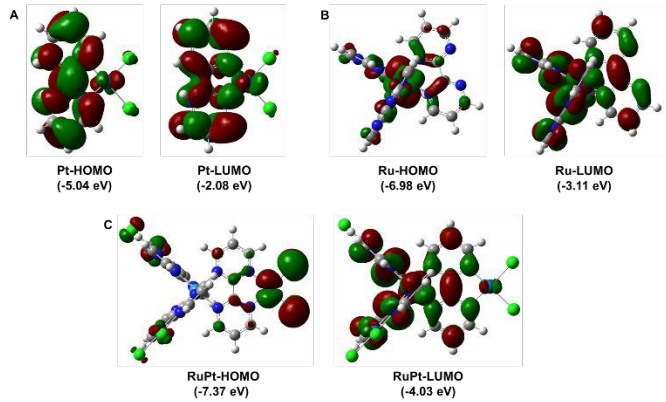

Figure 3. Molecular orbitals of (A) **Pt**, (B) **Ru** and (C) **RuPt** computed by DFT calculations in water using the PBE1PBE level of theory and 6-31+G(d) and LANL2DZ as basis sets.

The emissive properties of **Ru**, **Pt**, and **RuPt** upon excitation at 420 nm were investigated in water. The tetranuclear metal complex was found with a slight shift of the emission maximum to longer wavelength in comparison to its mononuclear components (**Pt**: 549 nm, **Ru**: 624 nm, **RuPt**: 638 nm; emission spectra: Figure S11). The Pt(II) complex **Pt** was poorly emissive with an emission quantum yield of 0.1%. In comparison, the Ru(II) polypyridine complex **Ru** (1.9%) and **RuPt** (0.4%) were stronger emissive. The ability of the complexes to catalytically generate singlet oxygen was assessed using the singlet oxygen probe 1,3-diphenylisobenzofuran. Singlet oxygen reacts with 1,3-diphenylisobenzofuran in a cycloaddition reaction, quenching its absorption peaks. By monitoring this quenching over time, the catalytic production of singlet oxygen was estimated.[13] **Ru**, **Pt**, and **RuPt** demonstrated to produce singlet oxygen upon light irradiation (Figure S12). Noteably, the mononuclear **Ru** complex was found to generate singlet oxygen more efficiently than the tetranuclear species.

The stability of a therapeutic agent is a critical parameter in determining its biological applicability. Previous studies have demonstrated that cisplatin derivatives remain stable in aqueous solution containing 0.9% sodium chloride; however, under conditions with lower chloride concentrations chloride ligands can be substituted.[14] Building on these previous findings, the stability of **RuPt** was evaluated in 0.9% sodium chloride solution by HPLC. After incubation for up to 48 h, no signs of decomposition were detected (Figure S13). Subsequently, the stability of **RuPt** in 0.9% sodium chloride solution upon exposure to red light at 630 nm was assessed. HPLC analysis indicated the generation of multiple species (data not shown). Matrix-assisted laser desorption ionization-time of flight mass spectrometry analyses suggested the release of several Pt(II) fragments from the tetranuclear **RuPt** complex (Release of one Pt fragment: calcd. for $C_{24}H_{18}Cl_5N_{12}Pt_2Ru$ $[M\text{-}PtCl_2\text{-}Cl]^+$ m/z 1140.8559; found: 1140.8561; Release of two Pt fragments: calcd. for $C_{24}H_{18}Cl_3N_{12}Pt_1Ru$ $[M\text{-}2PtCl_2\text{-}Cl]^+$ m/z 875.9534; found: 875.9531; Release of three Pt fragment: calcd. for $C_{24}H_{18}Cl_1N_{12}Ru$ $[M\text{-}3PtCl_2\text{-}Cl]^{2+}$ m/z 611.0509; found: 611.0506). Notebaly, previous studies have demonstarted the release of a Re(I) fragment from a bimetallic Ru(II)-Re(I) complex upon irradiation.[15]

The lipophilicity of the tetranuclear complex was evaluated by determining its distribution coefficient (logP) between phosphate-buffered saline and octanol using the shake-flask method. **RuPt** was detected primariyl in the octanol phase (logP = +2.3 ± 0.4), indicative of its high lipophilicity. Cell membrane permeability was further assessed using a parallel artificial membrane permeability assay (PAMPA). **RuPt** exhibited a medium permeability rate (0.017 ± 0.002 µm/s) in comparison to well-characterized reference compounds with known permeability values (Table S5).

Building on its promising photophysical and pharmacological characteristics, the therapeutic efficacy of **RuPt** was assessed in comparison with the clinically approved photosensitizer Photofrin and the chemotherapeutic drug cisplatin. The compounds were tested against cancerous mouse colon carcinoma (CT-26), human breast adenocarcinoma (MCF-7), and non-cancerous human fibroblast (GM-5657) cells. Cells were incubated with the compounds for 4 h, washed to remove non-internalized compounds, and subsequently irradiated with either blue light (450 nm, 20% power, 10 min, 1.2 J/cm²) or red light (630 nm, 10% power, 15 min, 0.9 J/cm²). After an addiitonal 44 h, cell viability was determined using a 3-(4,5-dimethylthiazol-2-yl)-2,5-diphenyltetrazolium bromide (MTT). assay. The mononuclear **Ru** complex was found to be non-toxic across all investigated cell lines, both under dark conditions and following irradiation (IC_{50} > 100 µM). Similarly, the **Pt** complex exhibited no toxicity in MCF-7 and GM-5657 cells and only a weak cytotoxic effect in CT-26 cells in the dark (IC_{50} = 42.3 ± 3.7 µM), which was marginally enhanced upon blue light irradiation ($IC_{50,blue}$ = 35.6± 4.1 µM). In contrast, the tetranuclear **RuPt** complex displayed notable dark toxicity in all examined cell lines (IC_{50} = 20.5-26.7 µM). Importantly, its cytotoxic response was enhanced upon light activation. Upon irradiation with blue light (IC_{50} = 5.3–13.6 µM) or red light (IC_{50} = 9.7–18.9 µM), the cytotoxic response was significantly enhanced compared to dark conditions. This

Table 1. IC_{50} values in µM of **Ru**, **Pt**, and **RuPt** in comparison to the clinically applied photosensitizer Photofrin and the chemotherapeutic drug cisplatin in mouse colon carcinoma (CT-26), human breast adenocarcinoma (MCF-7), and non-cancerous human fibroblast (GM-5657) cells in the dark or upon blue (450 nm, power: 20%, 10 min, 1.2 J/cm²) or red (630 nm, power: 10%, 15 min, 0.9 J/cm²) light irradiation. Three independent measurements as mean ± standard deviation. [a] = maximal solubility of Photofrin within cell media.

	CT-26			MCF-7			GM-5657		
	dark	450 nm	630 nm	dark	450 nm	630 nm	dark	450 nm	630 nm
Ru	>100	>100	>100	>100	>100	>100	>100	>100	>100
Pt	42.3 ± 3.7	35.6± 4.1	43.6 ± 4.7	>100	>100	>100	>100	>100	>100
RuPt	22.4 ± 1.8	6.2 ± 0.4	11.4 ± 0.6	20.5 ± 1.3	5.3 ± 0.5	9.7 ± 0.8	26.7 ± 1.2	13.6 ± 1.1	18.9 ± 2.3
Photofrin	>50[a]	3.8 ± 0.5	2.6 ± 0.4	>50[a]	3.5 ± 0.4	2.6± 0.2	>50[a]	4.3 ± 0.4	3.5 ± 0.6
cisplatin	7.1 ± 0.6	-	-	10.2 ± 0.7	-	-	12.4 ± 0.5	-	-

pronounced light-dependent increase in cytotoxcity demonstrates that the **RuPt** complex is photoactivatable, with blue light producing the strongest effect. The ability to trigger cytotoxicity under red-light irradiation is particularly noteworthy as red light penetrates tissues more deeply (overview: Table 1, drug-response curves. Figure S14).

For a deeper insight into the mechanism of action, particular due to release of the Pt(II) fragments from the tetranuclear Ru(II)-Pt(II) complex upon irradiation, the subcellular localization of the compound was studied by inductively coupled plasma optical emission spectroscopy. The cancer cells were incuated with **RuPt** for 4 h, washed to remove non-internalized compounds, the major cellular organelles were isolated, and the respective ruthenium and platinum metal content analyzed. The results revealed distinct subcellular distribution patterns for ruthenium and platinum. Both metals were predominantly localized in the cytoplasm. However, platinum accumulated in the nucleus, consistent with previous reports of platinum-based drugs. In contrast, ruthenium did not significantly accumulate in major organelles, including the nucleus, mitochondria, or lysosomes, but remained largely confined to the cytoplasmic compartment (Figure 4). Noteably, previous studies have shown the multitarget and multiaction effect of a bimetallic Ru(II)-Pt(IV) complex for multimodal anticancer therapy.[16]

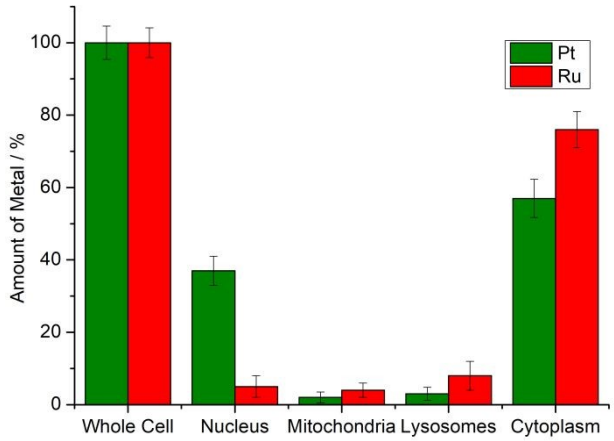

Figure 4. Subcellular localization of the metals Ru and Pt of the tetranuclear complex **RuPt** upon incubation with CT-26 cells after 4 h incubation in the dark, extraction of their cellular organelles and determination of the amount of each metal in each organelle by inductively coupled plasma optical emission spectroscopy.

In summary, this study describes the chemical synthesis, photophysical characterization, and biological evaluation of a novel tetranuclear Ru(II)–Pt(II) complex. Upon irradiation, the Pt(II) fragments are released, inducing a multimodal therapeutic effect. The Pt(II) species accumulate in the nucleus, triggering a chemotherapeutic response, while the Ru(II) moiety functions as a photosensitizer, generating singlet oxygen within the cytoplasm. This dual mechanism enables the tetranuclear Ru(II)–Pt(II) complex to exert potent phototoxic effects across a range of cancer cell lines at micromolar concentrations, highlighting its potential as a versatile agent for combined PACT and PDT. We are confident that this study will open new avenues for multimodal and multinuclear light activated anticancer therapy.

Data availability

The data supporting the findings of this study are available within the article and its supplementary information

Conflicts of interest

There are no conflicts to declare.

Acknowledgments

J. Karges gratefully acknowledges the financial support provided by the Liebig fellowship from the Chemical Industry Fund of the German Chemical Industry Association, the Life Sciences Bridge Award from the Aventis Foundation, and the Paul Ehrlich & Ludwig Darmstaedter Early Career Award 2024 – a prize awarded by the Paul Ehrlich Foundation, Germany.

References

1. D. E. J. G. J. Dolmans, D. Fukumura and R. K. Jain, *Nat. Rev. Cancer*, 2003, **3**, 380-387.
2. T. C. Pham, V.-N. Nguyen, Y. Choi, S. Lee and J. Yoon, *Chem. Rev.*, 2021, **121**, 13454-13619.
3. X. Zhao, J. Liu, J. Fan, H. Chao and X. Peng, *Chem. Soc. Rev.*, 2021, **50**, 4185-4219.
4. J. Karges, *Angew. Chem. Int. Ed.*, 2022, **61**, e202112236.
5. S. Monro, K. L. Colón, H. Yin, J. Roque, III, P. Konda, S. Gujar, R. P. Thummel, L. Lilge, C. G. Cameron and S. A. McFarland, *Chem. Rev.*, 2019, **119**, 797-828.
6. S. Bonnet, *J. Am. Chem. Soc.*, 2023, **145**, 23397-23415.
7. N. J. Farrer, L. Salassa and P. J. Sadler, *Dalton Trans.*, 2009, 10690-10701.
8. K. M. Kuznetsov, K. Cariou and G. Gasser, *Chem. Sci.*, 2024, **15**, 17760-17780.
9. H. Muramatsu, S. Shimada and T. Okada, *J. Biol. Phys.*, 2017, **43**, 355-365.
10. L. Yang, F. L. Wimmer, S. Wimmer, J. Zhao and P. S. Braterman, *J. Organomet. Chem.*, 1996, **525**, 1-8.
11. S. Campagna, F. Puntoriero, F. Nastasi, G. Bergamini and V. Balzani, in *Photochemistry and Photophysics of Coordination Compounds I*, eds. V. Balzani and S. Campagna, Springer Berlin Heidelberg, Berlin, Heidelberg, 2007, pp. 117-214.
12. H. Yin, M. Stephenson, J. Gibson, E. Sampson, G. Shi, T. Sainuddin, S. Monro and S. A. McFarland, *Inorg. Chem.*, 2014, **53**, 4548-4559.
13. A. Fennes, N. Montesdeoca, Z. Papadopoulos and J. Karges, *Chem. Commun.*, 2024, **60**, 10724-10727.
14. R. F. Greene, D. C. Chatterji, P. K. Hiranaka and J. F. Gallelli, *Am. J. Hosp. Pharm.*, 1979, **36**, 38-43.
15. Y. Wang, P. S. Felder, P. Mesdom, O. Blacque, T. L. Mindt, K. Cariou and G. Gasser, *ChemBioChem*, 2023, **24**, e202300467.
16. J. Karges, T. Yempala, M. Tharaud, D. Gibson and G. Gasser, *Angew. Chem. Int. Ed.*, 2020, **59**, 7069-7075.

View Article Online
DOI: 10.1039/D5CC05177K

Data availability

The data supporting the findings of this study are available within the article and its supplementary information